Proceedings of the 21st ICSMGE, Vienna, Austria, 14 – 19 June 2026. Pistrol, Adam & Schweiger (eds.)
Published by: ÖGG, Austrian Society for Geomechanics, Salzburg, Austria, ISBN 978-3-9503898-4-5
https://doi.org/10.53243/ICSMGE2026-1122

Numerical Modeling of Circular and Rectangular Shafts During Excavation and Microtunneling: Assessing the Impact of Jacking Forces on Structural Stability

Roshanak Shafieiganjeh, Grace Stapley, Frank Remmert
LF Consulting Engineers Austria GmbH, Vienna, Austria, roshanak.shafieiganjeh@ilf.com

ABSTRACT: This paper presents 2D and 3D numerical models of rectangular and circular shafts consisting of secant piles with the same geometrical setup and jacking forces. The modeling is focusing on the behavior of the shafts during excavation and micro tunneling within the scope of SuedLink project. The modelling approach implemented is used to assess the stability of the shafts and the deformation during the micro tunneling process. The numerical analysis presents the limitations in 2D modeling of the jacking force in rectangular shafts and provides insights into the optimization of design and the construction of similar infrastructure in challenging ground conditions.

KEYWORDS: Circular shaft, microtunneling, secant bored pile wall, finite element modeling.

1 INTRODUCTION

Pipe jacking is a micro tunneling method in which the lining of the resulting tunnel is pushed through the ground from the starting point rather than being built section-by-section behind the excavation face (Sterling, 2020). In the past century, many large pipe jacking projects have been conducted around the world (Wang et al., 2018). To reach the desired level of micro tunneling, start and target excavation pits should be designed. In the presence of groundwater, circular shafts made of reinforced concrete are used as jacking shafts. Circular shafts involving pre-installed diaphragm walls, bored piles and sheet piles have been excavated frequently in construction sites (Faustin et al., 2018). Among the different support systems, secant piles are constructed prior to excavation for ground retention. The wall is formed by constructing primary and secondary piles where the secondary ones cut into the primaries. In comparison to other support systems, secant piles are more flexible in shape and offer a more compact operation in limited urban spaces (Jin et al., 2020). Studies including the design, soil-pile interaction, and induced failure in secant pile wall circular shafts have been conducted by 3D finite element method (Chehadeh et al., 2015; Jin et al., 2020).

This paper focuses on the design of the secant pile wall circular shafts with high groundwater level as jacking shafts in SuedLink project and the stability of the shaft during the micro tunneling process. The SuedLink project is a significant high-voltage DC transmission network expansion designed as an underground cable connection in Germany. The jacking shafts in this project are designed to withstand the jacking force of up to 5000 kN. To assess the stability of the shafts, the horizontal deformation, and the forces transferred into the soil during micro tunneling, two models are executed using Plaxis 3D and Plaxis 2D. The 3D model represents the circular shaft. As the circular shaft cannot be modeled in the 2D plain strain condition, a substitute rectangular shaft with the same geometrical parameters is modeled to assess the 3D effect in applying the rather large jacking forces and the interactions of the soil-pile structure.

2 MODELING BASIS CONSIDERATIONS

2.1 *Geometry of the shaft*

The modeled jacking shaft is designed with an 8.8 m outer diameter including 0.9 m diameter piles. The depth of the shaft during the excavation phase reaches 8.6 m. A 1.2 m wide head beam with 0.8 m height is planned on top of the piles. The micro tunneling pipe is a DN 1600 with 1.6 m inner and 2.0 m outer diameter. To initiate the micro tunneling, a jacking abutment is designed on the top of the base slab with 1.0 m thickness, 4.7 m width and 3.5 m height. The configuration of the model is shown in Figure 1.

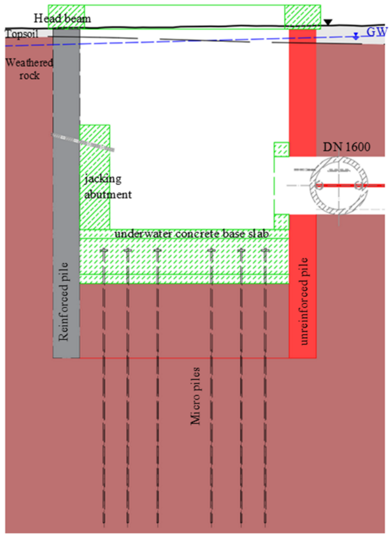

Figure 1. Configuration of the jacking shaft.

2.2 *Applied loads on the shaft*

According to German recommendations of the excavation pits (EAB, 2021), a 10 kN/m^2 constant load must be applied directly next to the shaft wall. In addition, a 40-ton crane load is applied as 125 kN/m^2 strip load on a 2.25 m wide surface directly next to the pit. A jacking force of 3500 kN is planned for micro tunneling which is applied on a 2.0 m · 2.0 m area on the jacking abutment.

2.3 *Design of the concrete base slab*

The failure of the excavation subjected to hydraulic uplift is assessed by German recommendations of the excavation pits (EAB, 2021).

$$V_{ds,k} \cdot \gamma_{G,ds} \leq G_{B,k} \cdot \gamma_{G,stb} \quad (1)$$

Where $V_{ds,k}$ is the hydrostatic water pressure on the base slab, $G_{B,k}$ is the dead weight of the overlying soil on the base slab, $\gamma_{G,ds}$ and $\gamma_{G,stb}$ are the partial safety factors equal to 1.1 and 0.95, respectively. Due to the groundwater at about 0.5 m below the surface level, the design of an anchored underwater concrete base slab with 1.2 m thickness and 30 cm leveling layers from bottom and top is required. The length calculated for micro piles based on EAB (2021) and Kinzler & Morgen (2014) is 8.0 m.

3 METHODOLOGY

Two numerical finite element models are conducted in this project using Plaxis software. The implemented modeling approach for the circular (3D) and rectangular (2D) models including assumptions and construction phases as well as the selected material models are presented herein.

3.1 *Numerical Model Development*

The secant bored pile wall is modeled as volume element. To present the stiffness of the head beam in the rectangular shaft (2D model), a strut with the same stiffness as concrete is modeled. As the piles are not reinforced in the radial direction, they cannot bear any tensile stress in this direction. To implement this concept in the 3D model, vertical interfaces are created along the whole length of the piles at the contact of each primary and secondary pile. In the circular shaft (3D model), an average distance equal to center-to-center distance of piles is assigned to these interfaces. Moreover, at the contact of each concrete part between jacking abutment and base slab, and piles and outer surface of the base slab a concrete-concrete interface is defined.

In order to read out the internal forces on the shaft wall, a plate element is provided in the middle of the piles. Plates are normally used to model thin structures in ground with considerable bending stiffness. However, the deformation of the shaft is here presented by the volume element. Therefore, a softening factor of 1000 is assigned to this plate to avoid implementation of any further stiffness into the model.

The jacking force is applied as a surface load in 3D model and line load in 2D model to the jacking abutment.

The models are meshed according to pre-defined refinements options in Plaxis software. The very fine meshes around the shaft area and fine meshes for the rest of the model are selected.

For design purposes, the jacking force is multiplied by partial factors. This results in convergence problems and load errors in the 2D model. In addition, due to the asymmetric nature of two-dimension models, an increased jacking force from micro tunneling would output an unsuitable design. This apparent exceedance of design tolerances would be evident by the significantly large and unrealistic forces and bending moments. To solve this problem, the 3D effect of the spatially limited passive earth resistance is considered. Following DIN 4085, the partial factor M μ_{pgh}^{res} is used for the increase in passive resistance of narrow foundation walls. This results in a lowering factor of 1.6 for jacking force in the 2D model.

$$E_{pgh}^{r} = \frac{1}{2} \cdot \gamma \cdot K_{pgh} \cdot \mu_{pgh}^{res} \qquad (2)$$

Where E_{pgh}^{r} is the passive earth resistance, K_{pgh} the passive earth pressure coefficient, and γ the unit weight of the soil. This post-processing would introduce a greater margin for error in the 2D model setup.

3.2 *Material models*

The ground model consists of a top-soil layer and weathered rock. The topsoil and weathered rock layer are modeled using the constitutive model ‘Hardening Soil’ to represent the deformation behavior and stiffness of material due to changes in the stress-state caused by unloading and reloading. The stiffness parameters are determined based on assumptions in Surarak et al., 2012. The interfaces are modeled using Mohr-Coulomb material model which can present the stress-strain behavior of rock layers. The concrete parts and the plate element are modeled using linear elastic model.

For the interfaces between the bored piles used to define the overlapping connection of each primary and secondary pile, the characteristic parameters for concrete are specified. This means that these interfaces (bored piles) can only withstand compressive forces.

The applied material parameters in the Plaxis software are summarized in Table 1.

Table 1. The applied material parameters in numerical models.

Parameter	Concrete	Plate	Interface piles	Interface concrete	Unit
γ	24.0*	0	25	0	kN/m^3
c			$7.5 \cdot 10^3$	0.01	kN/m^2
φ			27	1	°
ν	0.15	0.15	0.20		-
E_{intact}	$30.0 \cdot 10^6$	$30.0 \cdot 10^3$			kN/m^2
$E_{oedometer}$			$33.3 \cdot 10^6$	$30 \cdot 10^3$	kN/m^2

*For the underwater concrete base slab, 23 kN/m^3 is considered.

Parameter	Weathered rock	Topsoil	Unit
γ	23.0	16.0	kN/m^3
c	10.0	5.0	kN/m^2
φ	24	20	°
E^{ref}_{oed}	$35 \cdot 10^3$	$5 \cdot 10^3$	kN/m^2
E^{ref}_{50}	$35 \cdot 10^3$	$5 \cdot 10^3$	kN/m^2
E^{ref}_{ur}	$105 \cdot 10^3$	$15 \cdot 10^3$	kN/m^2
p^{ref}	100	100	kN/m^2
m	0.5	0.5	-
ν_{ur}	0.2	0.2	-

3.3 *Construction phases*

The numerical model must match the actual construction phases. Therefore, the following phases are carried out step by step in both 2D and 3D models:

- Initial calculations to achieve equilibrium.
- Construction of bored piles and head beam. In this phase the soft plate element, the interfaces between the primary and secondary bored piles and the interface between the shaft and the surrounding ground are activated.
- Activation of the constant and strip loads. The displacement is set to zero at the beginning of this phase.
- Underwater excavation to the bottom level of the underwater concrete base slab.
- Activation of the underwater concrete base slab and the interface around it.
- Drainage of the water from the shaft.
- Activation of jacking abutment and its bottom interface.
- Perforation of the piles through the 2.0 m diameter micro tunnel on opposite side of the jacking abutment in 3D model. This phase cannot be depicted in 2D model.
- Activation of jacking force on the jacking abutment (813 kN/m^2 in the 3D model and 515 kN/m^2 in the 2D model).

4 RESULTS

The results for stability and deformation represent the stability of the shaft and the impact of the forces acting on the structure during the micro tunneling process. The 3D model of the circular shaft demonstrated that the jacking forces of 3500 kN can be absorbed by the subsoil. This is shown through the following outputs.

4.1 *Deformation*

Deformation occurred after applying the jacking force is assessed on the soil model. For the rectangular shaft (2D model), the maximum deformation of 17.5 mm on the soil model is captured at the surface to approximately 4.0 m depth along the pile (Figure 2). However, for the circular shaft (3D model), the maximum deformation of 2.9 mm is captured at the head beam. The deformation at the contact of jacking abutment and concrete base slab reduces to 2.0 mm.

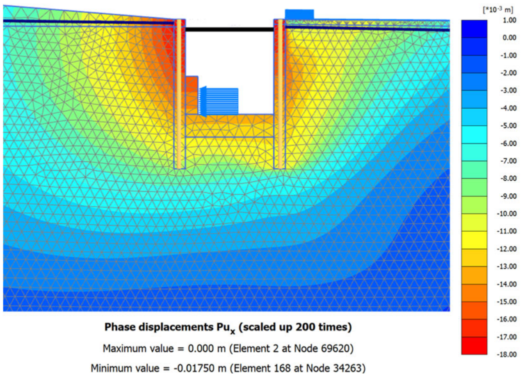

Figure 2. Horizontal displacement in x direction in rectangular shaft (2D model) in the construction phase of applying the jacking force.

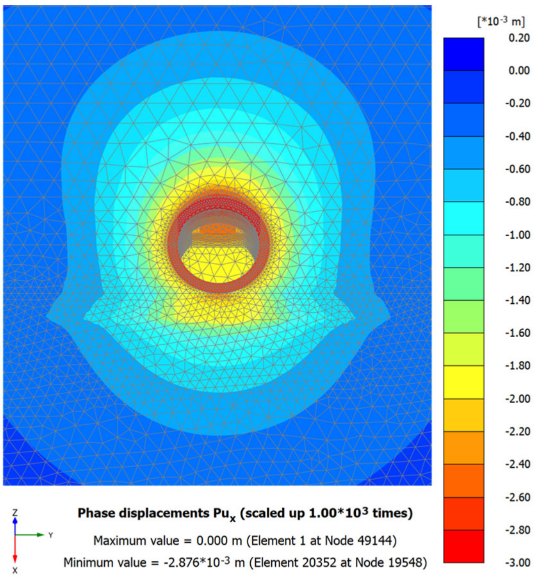

Figure 3. Horizontal displacement in x direction in circular shaft (3D model) in the construction phase of applying the jacking force.

4.2 *Forces*

To capture the forces acting on the bored piles, the vertical force (N1), bending moment (M), and shear force (Q) are measured in both 2D and 3D models. The radial force (N2) can be additionally obtained from the 3D model. The maximum and minimum values show the forces in the tensile (+) and compressive (-) directions. The results present the maximum negative and positive values of the forces acting on the plate element inside the shaft considering the 1000 softening factor from plate element, partial safety factors of constant influence of the temporary design situation (1.2), and the spacing of the reinforced piles only in the 3D model. As the 2D model represents an infinite section, the obtained forces can be considered per 1.0 m. The obtained forces from both models are summarized in Table 2. The forces obtained of the rectangular shaft model are larger than circular shaft, especially the bending moment. This means less required reinforcement for the circular shaft in comparison to the rectangular one.

Table 2. Measured forces acting on jacking shaft

Force	Rectangular shaft (2D)	Circular shaft (3D)	Unit
N1 (tensile)	620	309	kN
N1 (compressive)	761	533	kN
N2 (compressive)	-	1926	kN/m
M (Maximum)	409	53	kN.m
Q (Maximum)	339	166	kN

As is shown in Figure 4-a and 4-b, the maximum compressive vertical force is distributed around the micro tunnel opening area, and the maximum tensile axial force is captured where the jacking force is applied. However, the vertical forces on the rectangular shaft (2D model) are much larger than in the circular shaft (3D model) due to the limitation of the 2D model in distribution of the jacking force.

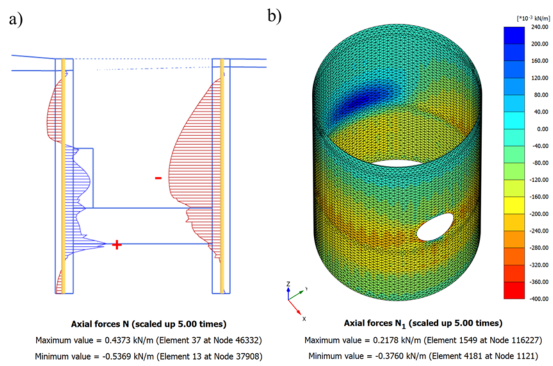

Figure 4. The acting vertical forces on the jacking shaft in a) rectangular shaft (2D model), and b) circular shaft (3D model).

According to Table 2, the compressive radial force obtained in 3D model of circular shaft is significantly large (Figure 5). Therefore, the ring compressive force transmission in the joint between the piles must be verified. The bearable radial force at the overlap height of the piles should be less than the compressive strength of concrete:

$$\mu = \frac{N_2/s}{f_{c,d}} \tag{3}$$

where μ is the utilization factor, s the overlap height of the piles, and $f_{c,d}$ the design value for the compressive strength of concrete. Considering a 0.48 m of overlap height, the utilization factor for radial force is at about 30 %.

According to Table 2, the bending moments and shear forces obtained from the rectangular shaft (2D model) are larger in comparison to the circular shaft (3D model). The bending moment and shear force can be obtained in 3D model in different bending and shear directions. The maximum Bending moment occurred at the micro tunnel opening area and jacking abutment on the opposite side in both 2D and 3D models. However, the maximum shear force is captured along the interfaces between the reinforced and unreinforced piles in the 3D model and around jacking abutment and concrete base slab in the 2D model. This highlights the effect of modeling structure of secant bored piles in the presented modeling setup.

5 DISCUSSION

The stability of the shaft during excavation and micro tunneling is impacted by the magnitude and transfer of the jacking forces, the interaction between the bored piles and the surrounding soil, and the internal structural response of the secant pile wall. The shaft stability is correlated to the deformation due to the forces acting on the secant pile wall. Throughout the excavation and after the application of the jacking force, the maximum horizontal deformations are considered acceptable. Any potential water ingress due to cracks, especially considering the low permeability of the rock (kf = 10^{-6} to 10^{-9}) and the presence of concrete thrust support, are considered manageable. Additionally, a friction-locked connection is suggested at the contact of underwater concrete base slab and bored pile walls.

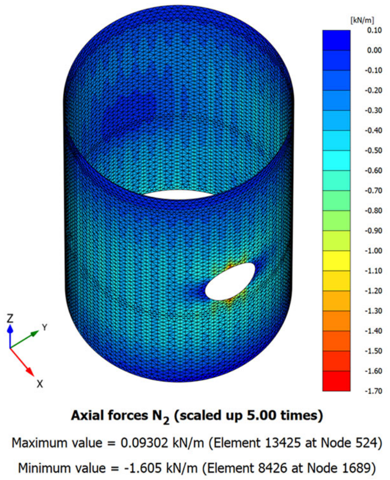

Figure 5. The acting radial force on the jacking shaft in the 3D model.

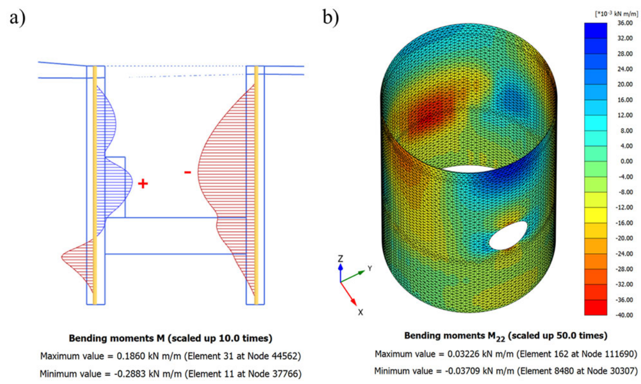

Figure 6. The acting bending moments on the jacking shaft in a) rectangular shaft (2D model), and b) circular shaft (3D model).

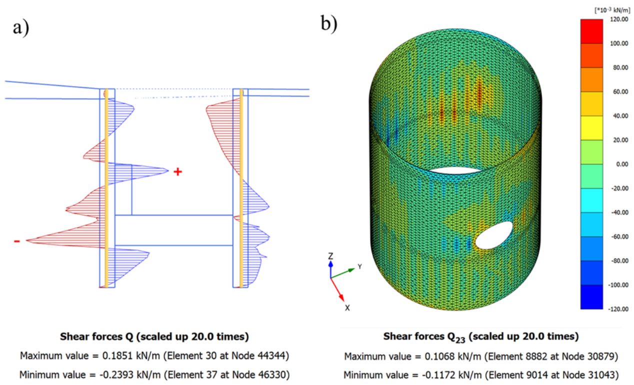

Figure 7. The acting shear forces on the jacking shaft in a) rectangular shaft (2D model), and b) circular shaft (3D model).

The comparison of the rectangular shaft in 2D and circular shaft in 3D models with an almost same setup showed some serious limitations of the 2D modeling approach in simulating the large jacking force. Some simplifications are carried out in the 2D setup such as skipping the construction phase of the perforation of the piles and factoring the applied jacking force to avoid obtaining unrealistic results. The limitations in modeling the geometry in a 2D setup such as ignoring the 4.7 m width of the jacking abutment results in the direct transfer of the jacking force into the wall and soil, instead of the transfer around the shaft, which overestimates the displacement and forces of the structure. In addition, the cutting forces between the piles, the radial load distribution with the help of jacking abutment cannot be modeled.

The 3D model of circular shaft illustrates how jacking forces transfer into the soil, creating a dynamic interaction that affects the shaft wall's structural response. Identifying the zones of maximum stress and deformation helps in optimizing the design to withstand these forces. The 3D model also provided insights into how the soil responds to the applied forces and how it supports the shaft structure.

Material models play a crucial role in numerical analyses. The geological properties of the presented trench in this paper allowed for implementation of Hardening-Soil constitutive model. This allows capturing the real stress-strain behavior of the soil during loading and unloading stages.

6 CONCLUSIONS

In this study, the behavior of a circular shaft and a rectangular shaft under a 3500 kN jacking force is assessed using 3D and 2D finite element numerical models, respectively. The 3D circular shaft model provides a more realistic representation of the jacking force transfer into the soil and captures the resulting deformations of the jacking abutment and secant pile wall more realistically compared to the 2D rectangular model. The 2D model of rectangular shaft overestimates the deformations and acting forces and results in a very conservative design. The findings highlight the utility of 3D numerical modeling for designing similar structures in complex ground conditions.

7 REFERENCES

EAB-Empfehlungen des Arbeitskreises „Baugruben“; Deutsche Gesellschaft für Geotechnik, 6. Auflage 2021.

Chehadeh, A., Turan, A., Abed, F., (2015). Numerical investigation of spatial aspects of soil structure interaction for secant pile wall circular shafts, Computers and Geotechnics 69, 452-461. http://dx.doi.org/10.1016/j.compgeo.2015.06.014

DIN 4085: Baugrund-Berechnung des Erddrucks, 2017-8.

Faustin, N.E., Elshafie, M.Z.E.B., Mair, R.J., (2018). Case studies of circular shaft construction in London, Proceedings of the Institution of Civil Engineers - Geotechnical Engineering 171, 391-404. https://doi.org/10.1680/jgeen.17.00166

Jin, D., Li, X., Yang, Y., Su, W., Wang, X., (2020). Stochastic analysis of secant piles failure induced by random imperfections, Computers and Geotechnics 124, 103640. https://doi.org/10.1016/j.compgeo.2020.103640

Kinzler, S., Morgen, K., (2014). Rückverankerte Betonsohlen-Nachweise in den Grenzzuständen UPL, GEO-2 und STR, Ernst & Sohn Verlag für Architektur und technische Wissenschaften GmbH & Co. KG, Berlin. Bautechnik 91, Heft 9. https://doi: 10.1002/bate.201400053

Sterling, R. (2020). Developments and research directions in pipe jacking and microtunneling. Underground space 5, 1-19. https:// doi.org/10.1016/j.undsp.2018.09.001

Surarak, C., Likitlersuang, S., Wanatowski, D., Balasubramaniam, A., Oh, E., Guan, H., (2012). Stiffness and strength parameters for hardening soil model of soft and stiff Bangkok clays. Soils Found. 52 (4), 682–697. https://doi.org/10.1016/J. SANDF.2012.07.009.

Wang, J., Wang, K., Zhang, T., Wang, S., (2018). Key aspects of a DN4000 steel pipe jacking project in China: A case study of a water pipeline in the Shanghai Huangpu River, Tunnelling and Underground Space Technology 72, 323-332. https:// doi.org/10.1016/j.tust.2017.12.012